

High-accuracy IMES Localization Using a Movable Receiver Antenna

Yoshihiro Sakamoto⁽¹⁾, Hiroaki Arie⁽²⁾, Takuji Ebinuma⁽³⁾, Kenjiro Fujii⁽⁴⁾, and Shigeki Sugano⁽⁵⁾

⁽¹⁾Waseda University, Tokyo, Japan: yoshi@aoni.waseda.jp

⁽²⁾RIKEN Brain Science Institute, Saitama, Japan: arie@bdc.brain.riken.jp

⁽³⁾The University of Tokyo, Tokyo, Japan: ebinuma@space.t.u-tokyo.ac.jp

⁽⁴⁾Hitachi Industrial Equipment Systems Co., Ltd., Tokyo, Japan: fujii-kenjiro@hitachi-ies.co.jp

⁽⁵⁾Waseda University, Tokyo, Japan: sugano@waseda.jp

Abstract—A method to improve positioning accuracy of an indoor messaging system (IMES) was introduced. With this method, Doppler shifts (produced by moving a receiver antenna) and three-axis attitude are used to determine the position of the receiver. A Doppler positioning system based on this method was developed and experimentally evaluated. The experimental results show that the method can achieve decimeter-level positioning accuracy.

Keywords—IMES; Doppler Positioning; Indoor Positioning

I. INTRODUCTION

Recently, especially in Japan, an “indoor messaging system” (IMES) is being developed as part of the indoor-positioning infrastructure [1]. IMES consists of transmitters that simply broadcast their fixed position by modulating it on the navigation message of a GPS-compatible signal. The main advantage of IMES is that off-the-shelf GPS receivers can be used with minor change to their firmware. However, since IMES does not use trilateration, unlike GPS or pseudolites, its positioning accuracy is limited to the installation interval of transmitters (normally 10-20 m). This accuracy is not an issue for the use of IMES with people; however, for robots, at least decimeter-level accuracy is necessary.

In the present work, a positioning method—called Doppler positioning—using a movable receiver antenna was developed. With this method, positioning is accomplished by using Doppler shifts, which are produced by moving an antenna, and three-axis attitude. Since trilateration is not used, positioning is possible even if the number of visible IMES transmitters is only one. The IMES infrastructure, which is constructed for use by people, can therefore also be used for robots without any modifications.

II. RELATED WORKS

In Antti's work [2], which is closely related to the present work, Doppler shifts brought by movement of satellites are used for calculating the position of the receiver. This idea originally derives from the “Transit system,” also known as NAVSAT, which was used for satellite navigation before GPS appeared [3].

Unlike satellite-based Doppler positioning, the positioning method used in the present work uses the Doppler shift produced by the receiver's movement. However, the equations used for calculating position are very similar to ones used for satellite-based Doppler

positioning. Accordingly, the positioning theory described in Section III-B is built upon Antti's work.

III. DOPPLER POSITIONING METHOD

We give an overview of the Doppler positioning using Fig. 1 as the reference before we get into the details. Two receivers are used to achieve Doppler positioning: one with a stationary antenna attached to the robot's body, and another with a movable antenna attached to the arm (whose position in the local coordinate system (LCS) is known) fixed to the robot. These two receivers are fully synchronized according to a single common clock. It is assumed that the robot remains stationary with respect to the world coordinate system (WCS), which gives the known position of the IMES transmitter. The procedure for determining the receiver's position (i.e., the origin of the LCS in terms of the WCS) is described in the following.

A. Acquisition of Doppler shift

Normally, a GPS receiver gives the carrier phase (also called Doppler count) ϕ at epoch t as

$$\phi(t+1) = \phi(t) + (f_{IN} - f_{L1})\Delta t + \varepsilon, \quad (1)$$

where f_{IN} is the frequency of an incoming carrier wave, f_{L1} is the nominal GPS L1 frequency, Δt is the time interval between each epoch, and ε is observational error. Here, f_{IN} includes receiver frequency bias δf , transmitter frequency bias δF , and Doppler shift produced by a change in the

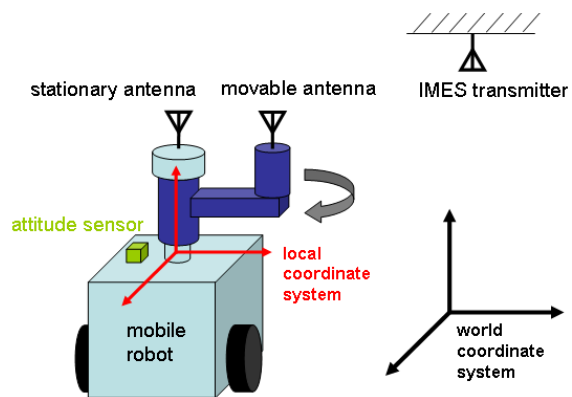


Figure 1. Overview of Doppler positioning system

geometric positions of the receiver and transmitter, f_{DOP} . Accordingly,

$$f_{IN} = \delta f + \delta F + f_{DOP} + f_{L1}. \quad (2)$$

If $\Delta\phi(t) = \phi(t+1) - \phi(t)$ is defined, (1) and (2) give

$$\Delta\phi(t) = (\delta f + \delta F + f_{DOP})\Delta t + \varepsilon. \quad (3)$$

It is assumed that there are two synchronized receivers, A and B, and A is moving while B remains still. The subtraction of (3) obtained from B from (3) from A is

$$\begin{aligned} \Delta\phi_{AB}(t) &= \Delta\phi_A(t) - \Delta\phi_B(t) \\ &= (\delta f + \delta F + f_{DOP})\Delta t \\ &\quad - (\delta f + \delta F)\Delta t + \varepsilon_{AB} \\ &= f_{DOP}\Delta t + \varepsilon_{AB} \end{aligned} \quad (4)$$

The relative geometric change of the moving receiver to the line-of-sight direction of transmitter at epoch t is

$$d(t) = \lambda_{L1}\Delta\phi_{AB}(t) = \lambda_{L1}f_{DOP}\Delta t + \varepsilon_d, \quad (5)$$

where λ_{L1} is the wavelength of the nominal GPS L1 carrier wave. Here, d in (5) is referred to as ‘‘delta range,’’ in a similar manner to that of the terminion of GPS.

B. Positioning of transmitter in LCS

The position of the IMES transmitter in the LCS is determined as follows. Fig. 2 shows the vector diagram for the position of a movable antenna, \mathbf{r}_a , the position of an IMES transmitter, \mathbf{r}_T , and the velocity of the movable antenna, \mathbf{v}_a . The observed delta range, d , acquired from (5), is expressed as

$$d = \mathbf{v}_a \cdot \frac{\mathbf{r}_T - \mathbf{r}_a}{\|\mathbf{r}_T - \mathbf{r}_a\|} + \varepsilon_d, \quad (6)$$

which is called an ‘‘observation equation’’ hereafter. If the antenna is moving during m epochs of time, m observation equations are acquired.

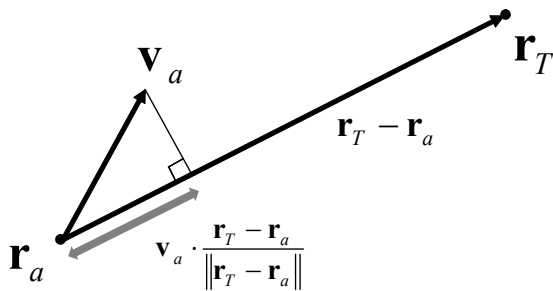


Figure 2. Vector expression for the position of a movable antenna and an IMES transmitter, and the velocity of the moving antenna in the LCS

To obtain \mathbf{r}_T with a redundant set of observation equations, a least-square method is used. However, since (6) is a non-linear function, the Newton-Raphson method (which is normally used for GPS) is used to linearize it as follows.

The non-linear term in (6) is first defined as

$$F(\mathbf{r}_T) = \mathbf{v}_a \cdot \frac{\mathbf{r}_T - \mathbf{r}_a}{\|\mathbf{r}_T - \mathbf{r}_a\|}. \quad (7)$$

If the initial value of the solution of \mathbf{r}_T is $\mathbf{r}_{T,0} = (x_0, y_0, z_0)$ and the second- and higher-order terms of the Taylor expansion of $F(\mathbf{r}_{T,0})$ are ignored, (6) is first updated as

$$\begin{aligned} d &= F(\mathbf{r}_{T,1}) + \varepsilon_d \\ &\approx \frac{\partial F(\mathbf{r}_{T,0})}{\partial \mathbf{r}_{T,0}} \Delta \mathbf{r}_{T,0} + F(\mathbf{r}_{T,0}) + \varepsilon_d \end{aligned} \quad (8)$$

If (8) is acquired for each observation k , namely, $k = 1$ to m , these equations are expressed as a matrix form.

$$\begin{bmatrix} \frac{\partial F_0^1}{\partial x_0} & \frac{\partial F_0^1}{\partial y_0} & \frac{\partial F_0^1}{\partial z_0} \\ \vdots & \vdots & \vdots \\ \frac{\partial F_0^m}{\partial x_0} & \frac{\partial F_0^m}{\partial y_0} & \frac{\partial F_0^m}{\partial z_0} \end{bmatrix} \begin{bmatrix} \Delta x_0 \\ \Delta y_0 \\ \Delta z_0 \end{bmatrix} = \begin{bmatrix} d^1 - F_0^1 \\ \vdots \\ d^m - F_0^m \end{bmatrix} + \varepsilon_d \quad (9)$$

The matrix of the left-hand side of (9) is defined as \mathbf{G} , called ‘‘geometry matrix’’ in GPS terminology, and the column vector of the right-hand side is defined as \mathbf{b} . Equation (9) is then expressed as

$$\mathbf{G}\Delta \mathbf{r}_{T,0} = \mathbf{b} + \varepsilon_d. \quad (10)$$

If the estimated value of $\Delta \mathbf{r}_{T,0}$ is denoted as $\Delta \hat{\mathbf{r}}_{T,0}$, the solution to (10) is

$$\Delta \hat{\mathbf{r}}_{T,0} = (\mathbf{G}^T \mathbf{G})^{-1} \mathbf{G}^T \mathbf{b}. \quad (11)$$

The estimated position is then updated according to

$$\hat{\mathbf{r}}_{T,1} = \mathbf{r}_{T,0} + \Delta \hat{\mathbf{r}}_{T,0}. \quad (12)$$

After this updating process is repeated several times, a sufficient approximate solution for the transmitter position is acquired.

C. Positioning of receiver in WCS

The origin of the LCS with respect to the WCS is defined as the position of the receiver (or robot in the example given in Fig. 1) and expressed as ${}^w \mathbf{r}_u$, which is the final value to estimate by the proposed Doppler positioning method. Here, superscript w of the vector

means WCS and l means LCS. Now, if the rotation matrix from the LCS to the WCS is defined as ${}^w\mathbf{R}_l$,

$${}^w\mathbf{r}_u = {}^w\mathbf{r}_T - {}^w\mathbf{R}_l {}^l\mathbf{r}_T \quad (13)$$

where ${}^w\mathbf{r}_T$ is the known transmitter position in the WCS, ${}^l\mathbf{r}_T$ is the transmitter position in the LCS, which is calculated in Section III-B, and ${}^w\mathbf{R}_l$ is determined using information from an attitude sensor.

In theory, it is unnecessary to use the LCS to determine the receiver's position in the WCS; its position can be directly calculated in the WCS from the beginning. To make the positioning theory clearer, however, in this paper, the LCS is used.

D. Dilution of precision

Under the Doppler-positioning scheme, as with the case of GPS, the magnitude of the estimated error is influenced by its geometry. From the general ideas of GPS [4], if it is assumed that the average of Doppler measurement error in (6) is zero, and its variance is σ_d^2 , the covariance matrix of $\Delta\mathbf{r}_{PL}$ in (10) is

$$\text{cov}(\Delta\mathbf{r}_{PL}) = \sigma_d^2 (\mathbf{G}^T \mathbf{G})^{-1} \quad (14)$$

If $(\mathbf{G}^T \mathbf{G})^{-1}$ is defined as \mathbf{H} , the dilution of precision (DOP) is expressed as the diagonal elements of \mathbf{H} .

$$\mathbf{H} = \begin{bmatrix} XDOP^2 & \bullet & \bullet \\ \bullet & YDOP^2 & \bullet \\ \bullet & \bullet & ZDOP^2 \end{bmatrix} \quad (15)$$

Here, XDOP means the DOP for the x-axis (likewise y- and z-axes). From (14) and (15), the variance of positioning error for each x-, y-, and z-axis is given by

$$\begin{aligned} \sigma_x^2 &= \sigma_d^2 XDOP^2 \\ \sigma_y^2 &= \sigma_d^2 YDOP^2 \\ \sigma_z^2 &= \sigma_d^2 ZDOP^2 \end{aligned} \quad (16)$$

Equation (16) shows that, as the value of DOP increases, the variance of the positioning also increases.

IV. POSITIONING EXPERIMENT

A. Purpose

The purpose of this experiment is to examine the achievable accuracy of the Doppler positioning and the influence of changing the condition under which the antenna is moved.

B. Devices for Doppler measurement

The same transmitter and receivers used in our previous pseudolite research were used [5]. The transmitter transmits a C/A code modulated on the GPS L1 band. As for the receiver, two receivers (SuperStar II from NovAtel Inc.) were modified so that they are synchronized with a common external clock (shown in Fig. 3). And a rotation-

type movable antenna unit (also shown in Fig. 3) was developed. This unit rotates the bar mounted on it clockwise and counterclockwise through a maximum of 360 degrees. A rotation-type antenna was chosen instead of linear-sliding type because it can generate two-dimensional movement with one degree of freedom.

C. Setup and procedure

Fig. 3 shows the experimental setup. The coordinates of the transmitter antenna and the origin of LCS (i.e., receiver's position) in terms of WCS are set to (0, 0, and 2680) and (0, -1500, and 920) in millimeters. In this experiment, an attitude sensor was not used, and it was assumed that all rotation angles of LCS with respect to WCS are known as zero (i.e., all directions of LCS are the same as those of WCS). The direction and inclination of the movable antenna unit was therefore carefully adjusted manually.

Two kinds of experiment (for convenience, called A and B.) were conducted. In experiment A, six measurements were conducted while the rotation radius of the movable antenna was varied, i.e., 300, 250, 200, 150, 100, and 50 (all in millimeters), with a 360-degree fixed rotation angle. In experiment B, six measurements were also conducted while the rotation angle was varied, i.e., 360, 180, 90, 45, 30, and 15 (all in degrees), with a 300-mm fixed rotation radius. For each measurement, the antenna was rotated clockwise and counter-clockwise alternately ten times with its rotation velocity and acceleration of 4 rpm and 4 rpm/s, respectively. The acquired data are the carrier phase and carrier-to-noise density ratio (C/N0) of the two receivers (stationary and moving ones) and current rotation angle.

D. Results

The position of the receiver in WCS was estimated from equations (1) to (13) off-line. Since the rank of the

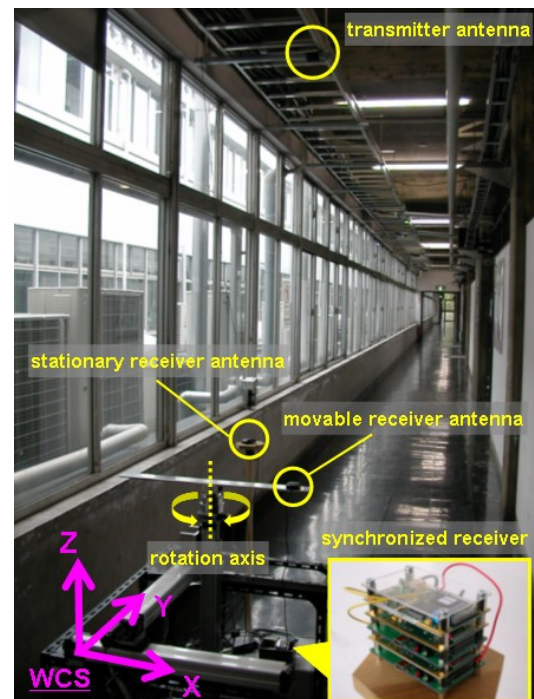


Figure 3. Experimental setup with a synchronized receiver and a rotation-type movable antenna unit

geometry matrix in (10) became two in all cases, the positions calculated were two-dimensional (x and y). Tables I and II list the results for experiments A and B. Symbols ΔX and ΔY mean the positioning error of the x- and y-axes, and "Error Norm" means square root. As clear from the tables, the error norm was smallest in the case of the longest rotation radius and the biggest rotation angle. However, the results show that the error norm did not monotonically increase as the radius and the angle became respectively shorter and smaller.

V. DISCUSSION

It is assumed that the rank of geometry matrix became two because the antenna was moved on the X-Y plane only. Fig. 4 shows scatter plots of row vectors of the geometry matrix in (10) when the rotation radius and angle are respectively 300 mm and 360 degrees. As clear from the graph, almost all plots are on the same plane, indicating that there are two linearly independent vectors; the rank of geometry matrix thus becomes two.

The influence of rotation radius and angle on the estimation error is discussed as follows. The DOP, which we defined in Section III-D, changes according to the geometric conditions. Basically, as the rotation radius and angle become, respectively, shorter and smaller, the values of the DOP become bigger (i.e., worse) because of smaller spatial diversity; consequently, the variance of positioning error becomes bigger.

There are two possible explanations for why the error norm in this experiment did not monotonically increase as the rotation radius and angle became shorter and smaller. First, the DOP is not the value of the positioning error but its variance. Accordingly, in consideration that the small number of measurements performed in this experiment (only once for each case), the true magnitude of error might not have been properly observed. Secondly, it is likely that some parameters that could affect the positioning accuracy changed according to the change of rotation radius and angle. For example, changing the rotation radius changed the velocity of the antenna

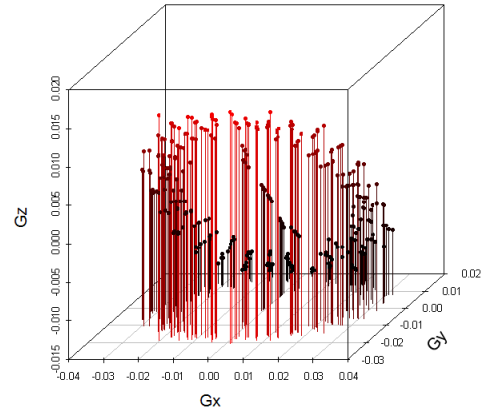


Figure 4. Scatter plots of row vectors of the geometry matrix when rotation radius and angle are 300 mm and 360 degrees

because the angular velocity was constant. Similarly, changing the rotation angle also changed the velocity of the antenna, especially in the cases of smaller antenna-rotation angles because of the influence of acceleration. In addition, in experiment B, the measurement time decreased as the rotation angle decreased. This condition affected the DOP because, if the length of measurement time becomes shorter, the number of rows of the geometry matrix decreases and then the values of DOP decreases. With these issues in mind, in future work, we will conduct more systematic experiments in which a single parameter can be controlled at a time.

VI. CONCLUSION

In this paper, it was assumed that the attitude of the movable antenna unit is known. If an attitude sensor is used, its measurement error will be added to the estimated position. However, this study shows that the Doppler-positioning method with a single IMES transmitter can achieve decimeter-level positioning accuracy.

REFERENCES

- [1] D. Manandhar, S. Kawaguchi, M. Uchida, M. Ishii, and H. Torimoto, "IMES for Mobile Users: Social Implementation and Experiments based on Existing Cellular Phones for Seamless Positioning", *Proc. of Int. Symposium on GPS/GNSS*, Tokyo, Nov. 2008.
- [2] Antti Lehtinen, "Doppler positioning with GPS," M.Sc. thesis, Tampere University of Technology, March 2002.
- [3] Pratap Misra and Per Enge, *Global Positioning System: Signals, Measurements, and Performance (Second Edition)*. Lincoln, MA: Ganga-Jamuna Press, 2006, pp. 19-21.
- [4] R.B. Langley, "Dilution of Precision," *GPS World*, Vol. 10, No. 5, pp. 52-9, May 1999.
- [5] Y. Sakamoto, H. Niwa, T. Ebinuma, K. Fujii, and S. Sugano, "Multiplexing receivers to improve positioning success rate for pseudolite indoor localization," *Proc. of 7th Int. Symposium on Mechatronics and its Applications (ISMA)*, Apr. 2010.

TABLE I

EXPERIMENT A: POSITIONING ERRORS FOR EACH ROTATION RADIUS

| Rotation Radius (mm) | ΔX (mm) | ΔY (mm) | Error Norm (mm) | C/N0 Mv. Ant. (dB-Hz) | C/N0 St. Ant. (dB-Hz) |
|----------------------|-----------------|-----------------|-----------------|-----------------------|-----------------------|
| 300 | -30.9 | -168.6 | 171.4 | 47.0 | 42.3 |
| 250 | -532.1 | -2.4 | 532.1 | 47.9 | 42.4 |
| 200 | -658.5 | 138.5 | 672.9 | 47.7 | 42.0 |
| 150 | -968.1 | 843.0 | 1283.7 | 47.2 | 42.0 |
| 100 | -147.1 | -295.1 | 329.8 | 46.4 | 41.5 |
| 50 | 496.5 | -531.8 | 727.5 | 44.6 | 40.8 |

TABLE II

EXPERIMENT B: POSITIONING ERRORS FOR EACH ROTATION ANGLE

| Rotation Angle (degree) | ΔX (mm) | ΔY (mm) | Error Norm (mm) | C/N0 Mv. Ant. (dB-Hz) | C/N0 St. Ant. (dB-Hz) |
|-------------------------|-----------------|-----------------|-----------------|-----------------------|-----------------------|
| 360 | -30.9 | -168.6 | 171.4 | 47.0 | 42.3 |
| 180 | 323.3 | -26.4 | 324.4 | 45.0 | 42.8 |
| 90 | -799.6 | 1759.2 | 1932.4 | 46.0 | 42.0 |
| 45 | 989.5 | -383.5 | 1061.2 | 45.6 | 41.5 |
| 30 | 1257.1 | -556.6 | 1374.9 | 48.6 | 41.9 |
| 15 | -623.0 | -591.5 | 859.1 | 45.5 | 41.4 |